Supporting Information

A Zwitterionic Metal-Organic Framework with Free Carboxylic Acid Sites that Exhibits Enhanced Hydrogen Adsorption Energies

Marianne B. Lalonde[a#], Rachel B. Getman[b,^#], Jeong Yong Lee[a,], John M. Roberts[a], Amy A. Sarjeant[a], Karl A. Scheidt[a], Peter A. Georgiev[c], Jan P. Embs[d], Juergen Eckert[e], Omar K. Farha[a,*], Randall Q. Snurr[b,*], Joseph. T. Hupp[a,*]

[#]*These authors made equal contributions.*

[a]*Department of Chemistry, Northwestern University, Evanston, Illinois 60208;*

[b]*Department of Chemical and Biological Engineering, Northwestern University, Evanston, Illinois 60208;*

[c] *Department of Structural Chemistry, University of Milan, 21 Via G. Venizian I-20133 Milano, Italy;*

[d] *Laboratory for Neutron Scattering, Paul Scherrer Institut, CH-5232 Villigen, Switzerland;*

[e] *Department of Chemistry, University of South Florida, 4202 East Fowler Avenue (CHE 205), Tampa, FL 33620*

[*]corresponding authors. E-mail: o-farha@northwestern.edu, snurr@northwestern.edu, j-hupp@northwestern.edu

^Present address: Department of Chemical and Biomolecular Engineering, Clemson University, Clemson, SC 29634-0909

Introduction

In this work we report the structures and H_2 storage properties of two zwitterionic MOFs, **NU-301** and **NU-302**. These structures feature zwitterionic characteristics arising from positively charged azolium groups on the linkers and negatively charged $Zn_2(CO_2)_5$ nodes.

Experimental Details

Activation

MOFs **NU-301** and **NU-302** were activated by first exchanging dimethylformamide with ethanol in an overnight soxhlet extraction. Following solvent exchange, the MOFs were heated under vacuum at 100 °C for 48 hours.

Sorption Experiments

All isotherms were measured on a Micromeritics TriStar II 3020. N_2 sorption was measured at 77 K, and H_2 was measured at both 77 K and 87 K. Hydrogen Qst was calculated using Virial analysis. (Figure S1.) BET surface area and pore volume were calculated using Micromeritics TriStar software. (Figure S2.)

Elemental Analysis

Elemental analyses of activated **NU-301 (**$C_{40}H_{26}N_2O_{13}Zn_2$). Calculated: C 55.01 %, H 3.01 %, N 3.21 %, O 23.8 %. Found: C 49.03 %, H 3.38 %, N 2.88 %, O 24.37 %, (averages from multiple analyses) Cl is found in trace levels (<0.25%). For **NU-302** ($C_{40}H_{25}BrN_2O_{13}Zn_2$) Calculated: C 50.43 %, H 2.65 %, N 2.94 %, Br 8.39 %. Found: C 46.56 %, H 2.98 %, N 3.21 %, Br 8.94 %, (averages from multiple analyses) Cl is found in trace levels (<0.25%).

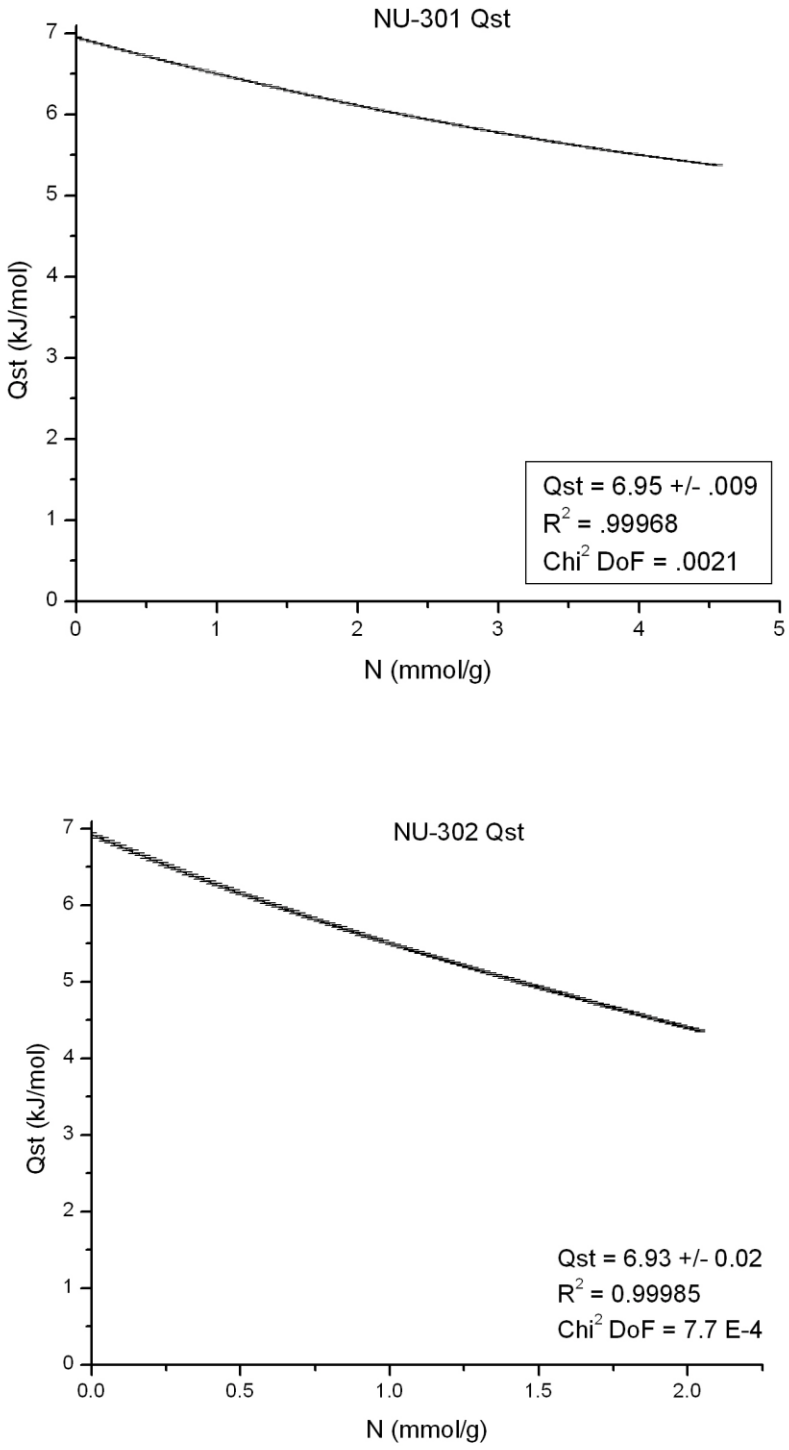

Figure S1: Qst plots for **NU-301** (top) and **NU-302** (bottom) including R^2, Chi^2DoF values and error bars.

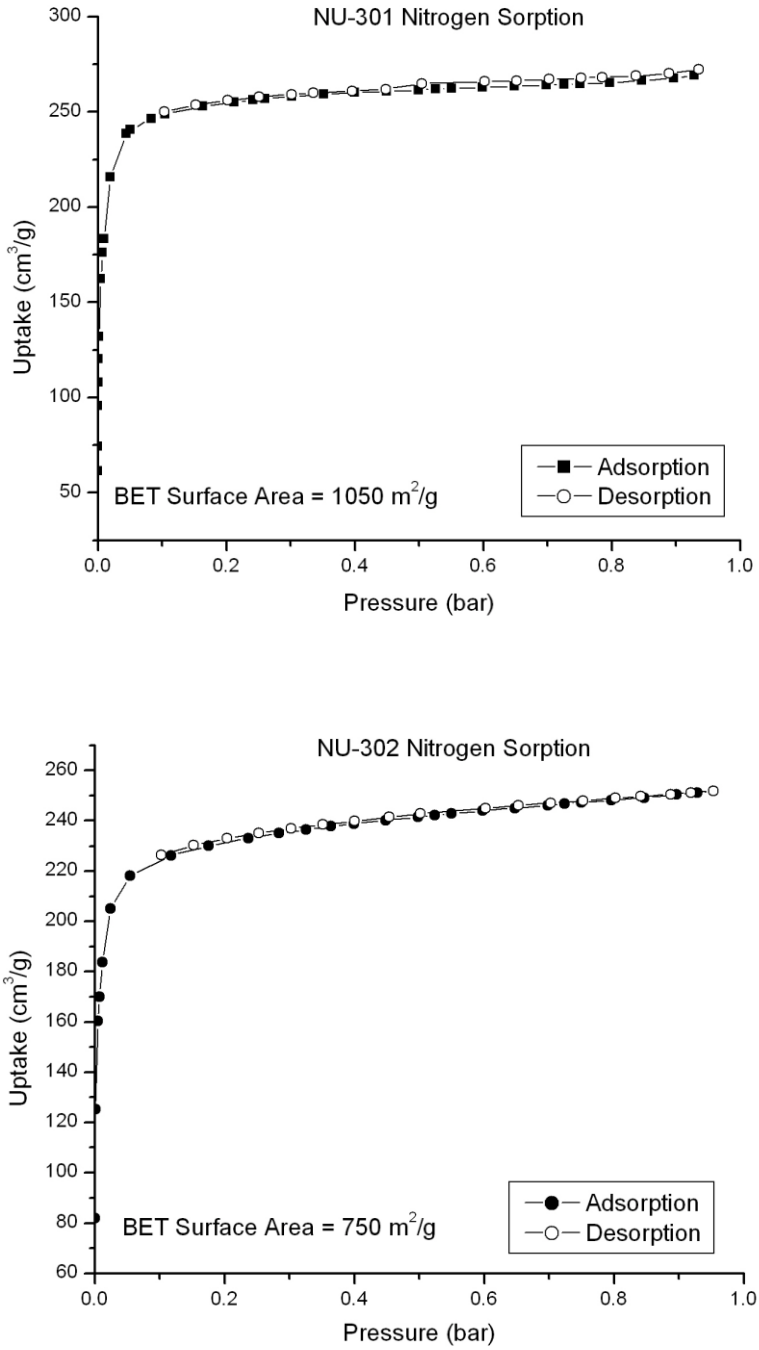

Figure S2: Nitrogen sorption plots for **NU-301** (top) and **NU-302** (bottom) including BET values

NMR Data

^{1}H NMR spectra were recorded on a Bruker 500 MHz NMR spectrometer with cryoprobe. Data are reported as ap = apparent, s = singlet, d = doublet, t = triplet, q = quartet, m = multiplet, b = broad; coupling constant(s) in Hz; integration was calculated using iNMR software. About 10 mg of MOF was dissolved in 1 mL of D_2O/D_2SO_4, sonicated, and transferred to NMR tube. Chemical shifts are reported in ppm (δ) and referenced to TMS. **NU-301**: ^{1}H NMR (500 MHz, D_2O/D_2SO_4) δ 8.24 (s, 1 H), 7.44 (d, 8 H), 7.08 (d, 2 H); 6.99, (d, 2 H); 6.82 (d, 8 H); 1.75 (s, 12 H). **NU-302**: ^{1}H NMR (500 MHz, D_2O/D_2SO_4) δ 8.24 (s, 1 H); 7.37 (d, 8 H), 7.08 (d, 2 H); 6.75 (d, 8 H); 1.75 (s, 12 H)

Characterization of the Zwitterionic MOFs

Single crystals of **NU-301** and **NU-302** were mounted in oil on glass fibers and placed in the nitrogen cold stream (100 K) of a Bruker AXS APEX2 diffractometer equipped with a CCD detector and graphite monochromated CuKα radiation. All data were corrected for absorption via SADABS. Structures were solved and refined using the SHELXTL suite of software. The program SQUEEZE (Platon) was used to remove electronic contributions from solvent molecules for each structure. See supporting CIF files for further refinement details.

Table S1. Crystal data and structure refinement for **NU-301** and **NU-302**

	NU-301	**NU-302**
Empirical formula	C199 H219 N21 O61	C55 H59 Br N7 O18
Formula weight	Zn8	Zn2
Volume	4403.91	1316.74
Temperature	100(2) K	100(2) K
Crystal system	Monoclinic	Triclinic
Space group	C2/m	P-1
Unit cell dimensions	a = 14.8149(18)Å b = 54.114(6)Å c = 9.2584(12)Å α = 90º β = 110.055(9)º γ = 90º	a = 9.2506(6) Å b = 14.4032(10)Å c = 27.384(2) Å a = 97.587(6) º b = 93.139(6) º g = 106.920(5) º
Volume	6972.3(15) $Å^3$	3443.4(4) $Å^3$
Z	8	2
Calculated density	1.049 mg/m^3	1.270 mg/m^3
Absorption coefficient	1.298 mm^{-1}	2.094 mm^{-1}
Goodness-of-fit on F^2	0.622	0.911
Final *R* indices[I>2sigma(I)]	R1 = 0.0953, wR2 = 0.2167	R1 = 0.0903, wR2 = 0.2221

PXRD patterns of as-synthesized samples (i.e. solvent-containing) are in good agreement with the single crystal data, while outgassed samples show large intensity drops of the main peak position around 3.1 at 2θ; see Figure S3.

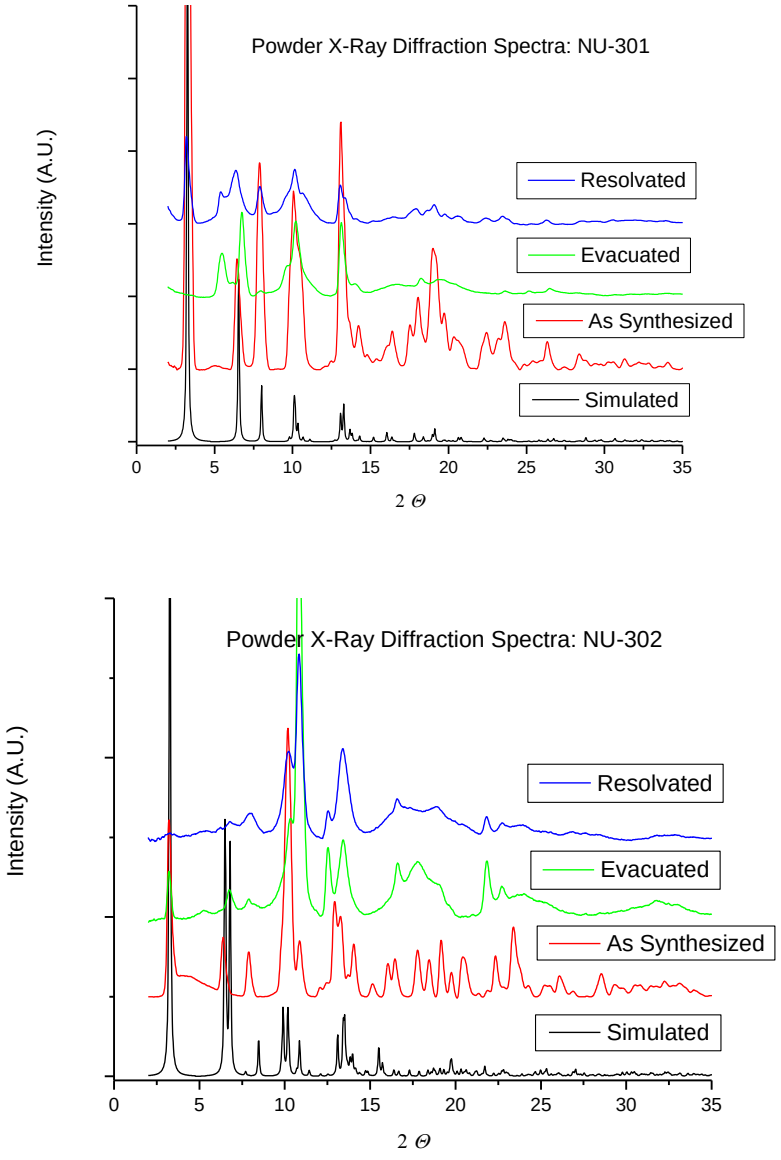

Figure S3. PXRD patterns of **NU-301** (top) and **NU-302** (bottom). From bottom to top, the plots correspond to patterns simulated from single-crystal data, experimental "as-synthesized" samples, experimental "solvent evacuated" samples, and experimental re-solvated samples. The experimental plots are background corrected.

Structural Data

Thermogravimetric analysis (TGA) was performed on a Mettler Toledo TGA/SDTA851 interfaced with a PC using Star software. Samples were heated at a rate of 10 ºC/min under a nitrogen atmosphere. (Figure S4.)

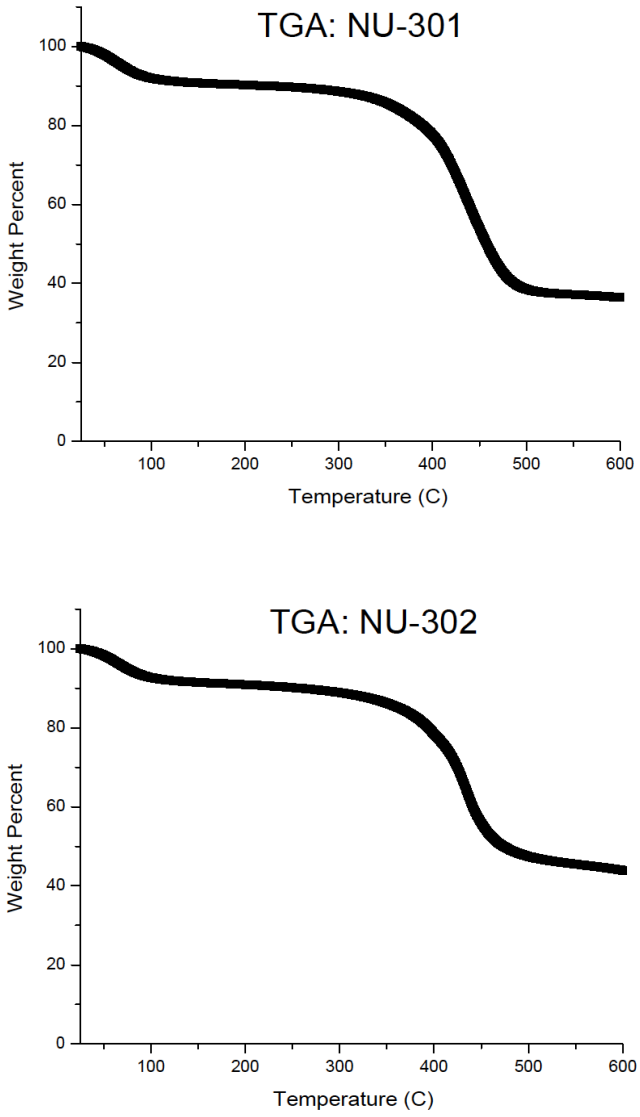

Figure S4. TGA Spectra of activated **NU-301** (top) and **NU-302** (bottom).

Computational Details

Electronic Structure Calculations

Electronic structure calculations were performed with the VASP code.[1] This code efficiently calculates the electronic structures of periodic systems using planewave basis sets. We used the projector augmented wave (PAW) method[2,3] to describe interactions between valence and frozen core electrons and the PBE[4] implementation of the generalized gradient approximation (GGA) to calculate electron exchange and correlation. Plane waves up to an energy cut-off of 449.69 eV were used to calculate the kinetic energies of the electrons. We used a 3x2x1 Monkhorst-Pack[5] **k**-point mesh to sample the first Brillouin zones. Electronic structures were performed self-consistently and were considered to be converged when the difference in electronic energy between subsequent interations feel below 10^{-3} eV. Partial charges on framework atoms were calculated using the density derived electrostatic and chemical (DDEC) charges method[6], which is an "atoms-in-molecules" method that assigns a portion of the total electron density to each individual atom and then compares assigned densities to reference densities in order to compute the charge.

H_2/Framework Interactions for Classical Simulations

Classical simulations were performed with our in-house multipurpose code RASPA[7]. Positions of framework atoms were taken from crystallography and held fixed throughout the simulations. The H_2 molecule was assumed to be rigid with a bond length of 0.741 Å.

H_2 interactions with framework atoms were calculated using a Lennard-Jones plus Coulomb potential. Lennard-Jones potentials employed DREIDING parameters[8] for framework atoms

and empirically derived parameters[9] for H_2. Cross-term Lennard-Jones parameters were obtained using the Lorentz-Berthelot mixing rules and are listed in Table S2. Interactions between H_2 molecules were calculated using Lennard-Jones potentials with the same empirically derived parameters for H_2. All Coulomb interactions were computed using DFT-calculated partial charges for framework atoms and the Darkrim-Levesque model[10] for H_2, which places charges of +0.468 at the H nuclei and a −0.936 charge at the center of mass in order to simulate the quadrupole. Using the Darkrim-Levesque model in coordination with the empirically derived Lennard-Jones parameters for H_2 has been shown previously to overestimate H_2 storage in charged frameworks,[11] and this likely contributes to the differences in the calculated and experimentally derived adsorption energies. However, to our knowledge there is no more suitable model for describing both electrostatic and dispersive and repulsive interactions. Coulomb interactions between H_2 molecules were neglected in all cases.[9]

Table S2. Lennard-Jones parameters used to describe H_2/framework atom dispersion and repulsion interactions in classical simulations.

MOF atom (X)	$\sigma_{H2\text{-}X}$ **(Å)**	$\varepsilon_{H2\text{-}X}/k_B$ **(K)**
Zn	3.499	31.884
C	3.214	41.910
H	2.904	16.756
O	2.994	42.054
N	3.109	37.818
Br	3.239	82.687
H_2	2.958	36.7

Computational Results

Partial Charges on Framework Atoms

Calculated partial charges on framework atoms in **NU-301** and **NU-302** are given in Tables S4 and S5. Summing from these tables, the $Zn_2(CO_2)_5$ nodes exhibit charges of −1.02, and the imidazole rings exhibit charges of +0.53. The separation of charges in this zwitterionic MOF is thus between these two groups.

Table S4. Calculated partial charges on framework atoms in **NU-301**.

	Description	occurance	Calculated Charge
Zn		8	1.032
N		8	0.129
H_i	instead of Br	4	0.124
C_a	methyl groups (IMTA)	16	-0.401
C_b	to imidazole ring (IMTA)	8	-0.069
C_c	to methyl groups (IMTA)	16	0.161
C_d	benzene ring (IMTA)	8	-0.014
C_e	to COO (IMTA)	16	-0.171
C_f	imidazole ring (IMTA)	12	-0.074
C_g	COO (IMTA)	8	0.698
C_h	COO with free O (IMTA)	8	0.657
C_i	center ring, to Br (BTBA)	4	-0.183
C_j	on center ring (BTBA)	4	0.017
C_k	on center ring (BTBA)	4	0.033
C_l	to center ring (BTBA)	4	0.105
C_m	on “free” COO ring (BTBA)	8	-0.161
C_n	to “free” COO (BTBA)	4	-0.146
C_o	on “free” COO ring (BTBA)	8	-0.039
C_p	“free” COO (BTBA)	4	0.633
C_q	to center ring (BTBA)	4	0.090
C_r	on “bound” COO ring (BTBA)	8	-0.167
C_s	to “bound” COO (BTBA)	4	-0.137
C_t	on “bound” COO ring (BTBA)	8	-0.038
C_u	“bound” COO (BTBA)	4	0.692
H_a	methyl groups (IMTA)	48	0.134
H_b	imidazole ring (IMTA)	12	0.167
H_c	to C_d (IMTA)	8	0.124
H_d	to C_m	8	0.121
H_e	to C_o	8	0.100
H_f	to C_r	8	0.113
H_g	to C_t	8	0.122
H_h	free COO (BTBA)	4	0.412
O_a	COO (IMTA)	16	-0.610
O_b	COO, free (IMTA)	8	-0.576
O_c	COO with free O, to Zn (IMTA)	8	-0.603
O_d	COO, free (BTBA)	8	-0.525
O_e	COO (BTBA)	8	-0.603

Table S5. Calculated partial charges on framework atoms in **NU-302**.

	Description	occurance	Calculated Charge
Zn		4	1.007
N		4	0.121
Br		2	-0.054
C_a	methyl groups (IMTA)	8	-0.401
C_b	to imidazole ring (IMTA)	4	-0.062
C_c	to methyl groups (IMTA)	8	0.147
C_d	benzene ring (IMTA)	4	-0.018
C_e	to COO (IMTA)	8	-0.164
C_f	imidazole ring (IMTA)	6	-0.071
C_g	COO (IMTA)	4	0.693
C_h	COO with free O (IMTA)	4	0.663
C_i	center ring, to Br (BTBA)	2	0.026
C_j	on center ring (BTBA)	2	-0.013
C_k	on center ring (BTBA)	2	-0.011
C_l	to center ring (BTBA)	2	0.099
C_m	on “free” COO ring (BTBA)	4	-0.163
C_n	to “free” COO (BTBA)	2	-0.123
C_o	on “free” COO ring (BTBA)	4	-0.033
C_p	“free” COO (BTBA)	2	0.632
C_q	to center ring (BTBA)	2	0.088
C_r	on “bound” COO ring (BTBA)	4	-0.165
C_s	to “bound” COO (BTBA)	2	-0.124
C_t	on “bound” COO ring (BTBA)	4	-0.034
C_u	“bound” COO (BTBA)	2	0.684
H_a	methyl groups (IMTA)	24	0.132
H_b	imidazole ring (IMTA)	6	0.168
H_c	to C_d (IMTA)	4	0.123
H_d	to C_m	4	0.117
H_e	to C_o	4	0.110
H_f	to C_r	4	0.113
H_g	to C_t	4	0.116
H_h	free COO (BTBA)	2	0.409
O_a	COO (IMTA)	8	-0.599
O_b	COO, free (IMTA)	4	-0.579
O_c	COO with free O, to Zn (IMTA)	4	-0.601
O_d	COO, free (BTBA)	4	-0.528
O_e	COO (BTBA)	4	-0.590

Inelastic Neutron Scattering Studies

We have observed the hindered rotor transitions of H_2 adsorbed at various loadings by inelastic neutron scattering in both **NU-301** and **NU-302** in order to gain more information on the numbers and types of binding sites available in the two materials. The transition between the lowest two levels of the hindered rotor results from rotational tunneling, and its frequency is therefore extraordinarily sensitive to the height and shape of the barrier to rotation. A lower frequency indicates a higher barrier to rotation, which in turn is likely to arise from a stronger interaction at that particular binding site.

A detailed assignment of these rotational spectra requires either the use of an appropriate phenomenological model of the rotational potential energy surface and transitions associated with it, or explicit quantum dynamical calculations of the rotational energy levels on the *ab-initio* potential energy surface (PES). Such calculations, however, are very involved because it is extremely difficult to obtain a PES of sufficient accuracy to account properly for the quantum dynamics of the adsorbed hydrogen molecule.[13] We have therefore taken the simplest phenomenological model for the hindered rotations, one of 3D reorientation in a double-minimum potential,[14] for a preliminary interpretation of our data. Within this model most of the peaks in the lower part of the energy range of this experiment can then be assigned to a "0-1" transition, each of which must then originate from a hydrogen molecule on a different binding site.

INS spectra were obtained with a fixed incident energy of 20.4 meV, (2.0 Å), which limited the maximum energy transfer for neutron energy loss to about 16.5 meV. Neutron energy gain (negative energy, i.e. energy loss by the sample) spectra are remarkably rich, which suggests that spin conversion is not rapid, as expected in the absence of paramagnetic ions or impurities. Hydrogen molecules bound to the organic linker sites with transitions near the free rotor value of 14.7 meV apparently do exhibit spin conversion, as the strong peaks above 12 meV do not appear in the energy gain spectra.

The neutron energy gain spectra (Figure S3, bottom) for both compounds exhibit, roughly speaking, three rather broad features at and below 10 meV, which may be attributed to the three types of strong binding sites found in our computational work. The lowest rotational tunneling transitions in neutral MOFs without open metal sites tend to be above 10 meV,[15] so this observation qualitatively supports the higher values of Q_{st} for our compounds. The width of the bands is typical for systems with charged frameworks,[16] or with ionic species, and reflects the fact that the binding sites for H_2 may be quite heterogeneous in the vicinity of the charges. The width may, of course, also reflect a degree of structural disorder in the framework.

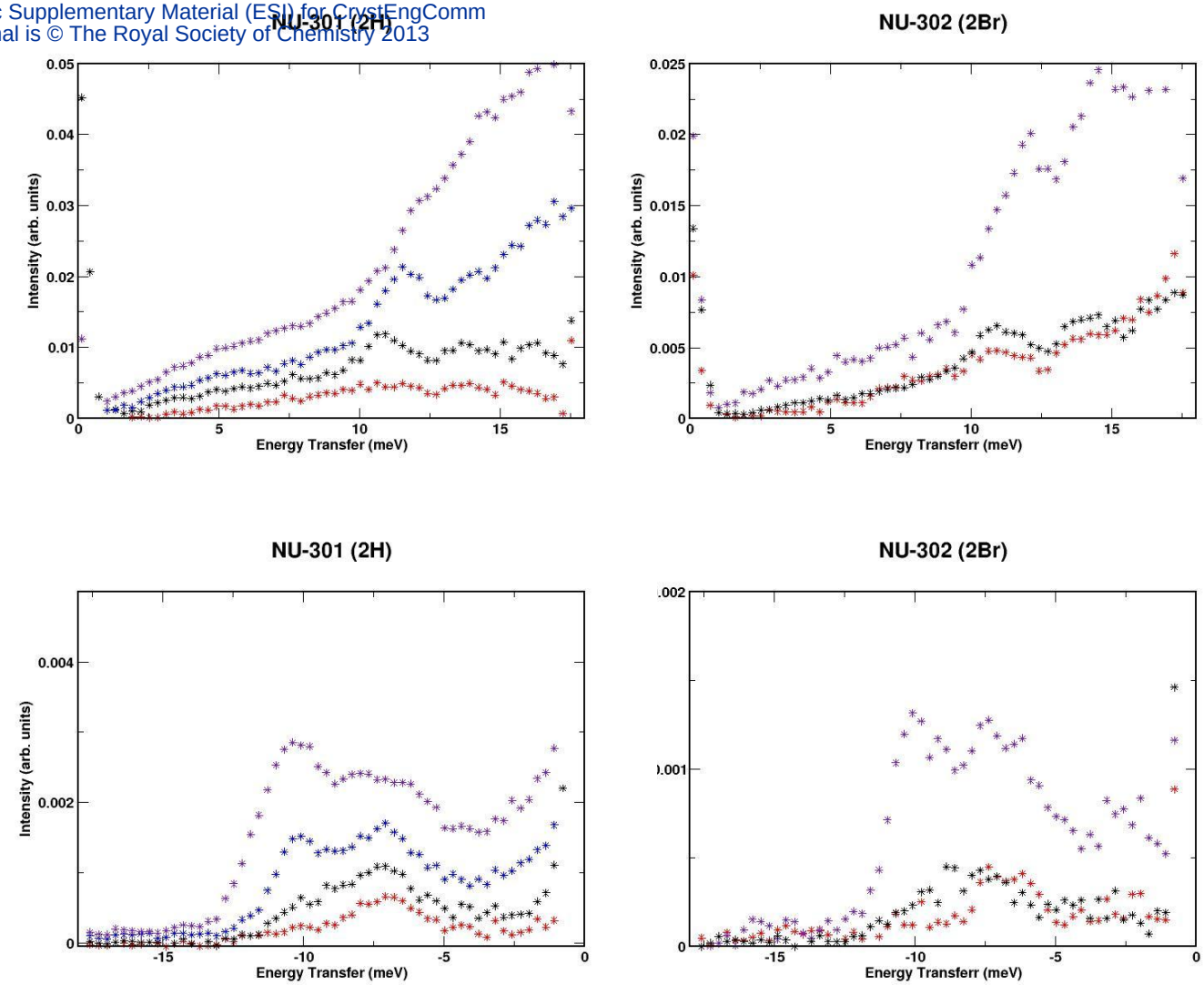

Figure S3. INS spectra for neutron energy loss, (top), and energy gain (de-excitation of rotational levels, bottom) at T=1.5 K for H2 in **NU-301** (left) and **NU-302** (right). The respective background spectrum was subtracted in each case. Hydrogen loadings were 2.3(red), 4.7(black), 8.7 (blue) and 22 mmol (purple) in **NU-301**, 2 (red), 3 (black) and 10 mmol (purple) in **NU-302**. Relative hydrogen loadings were similar (see Table S6) and 22 mmol (purple) in **NU-301**, 2 (red), 3 (black) and 10 mmol (purple) in **NU-302**. Relative hydrogen loadings were similar (see Table S6).

The INS Spectra for **NU-301** and **NU-302** appear to be rather similar, as they reflect similar binding sites, and show peaks at approximately 6.5, 8 and 10.5 meV. Only the first two of these have appreciable intensities (and hence population of the respective binding sites), while the peak at about 10.5 meV only gains appreciable intensity at higher loadings, and this more so in **NU-302** than in **NU-301**. We may associate the two peaks at the lower energies (= higher barriers to rotation) with the two high-energy binding sites, i.e. the "zwitterionic" and

"carboxylic acid" sites in **NU-301** and **NU-302**. The broad band between 10 and 11 meV must then result from some of the H_2 molecules bound around the "carboxylic acid/node" sites, which also seem to contribute a very broad underlying background intensity on account of the wide range of binding modes around those sites. Weak binding sites on the organic parts of the linkers become occupied at the highest loadings as is evident from the very strong intensity within about 1 meV of the free rotor transition (14.7 meV). The highest loadings we used were achieved at temperatures well below 77 K and correspond to elevated pressures at 77 K.

The above observations are in accord with the fact that we find no difference in binding energies of H_2 in **NU-301** and **NU-302**. Difference spectra (Figure S4,) do, however, reveal some additional, relatively small peaks at low energy (high barrier to rotation) in NU-301. These peaks may indicate the presence of some stronger binding sites in this material, which may, however, be too small in number to be reflected in the average thermodynamic properties. The peaks at +/- 4 meV are in fact rather close in energy to those for H_2 at some of the strongest binding sites at extra framework cations in zeolites.[17] The direct comparison (Figure S4, left) of the spectra for **NU-301** and **NU-302** also shows that the former has greater intensity at lower energies (stronger binding), which seems to be balanced by stronger scattering at higher energies in the latter.

It would be of considerable interest to relate these qualitative observations to the actual binding sites in the two materials, the attendant barriers to rotation, and their rotational transitions. It is not clear, however, that the required calculations can at this time be performed with sufficient accuracy mainly because of the difficulty of obtaining a potential energy surface, which reflects all the subtleties of the interactions of hydrogen with the host.

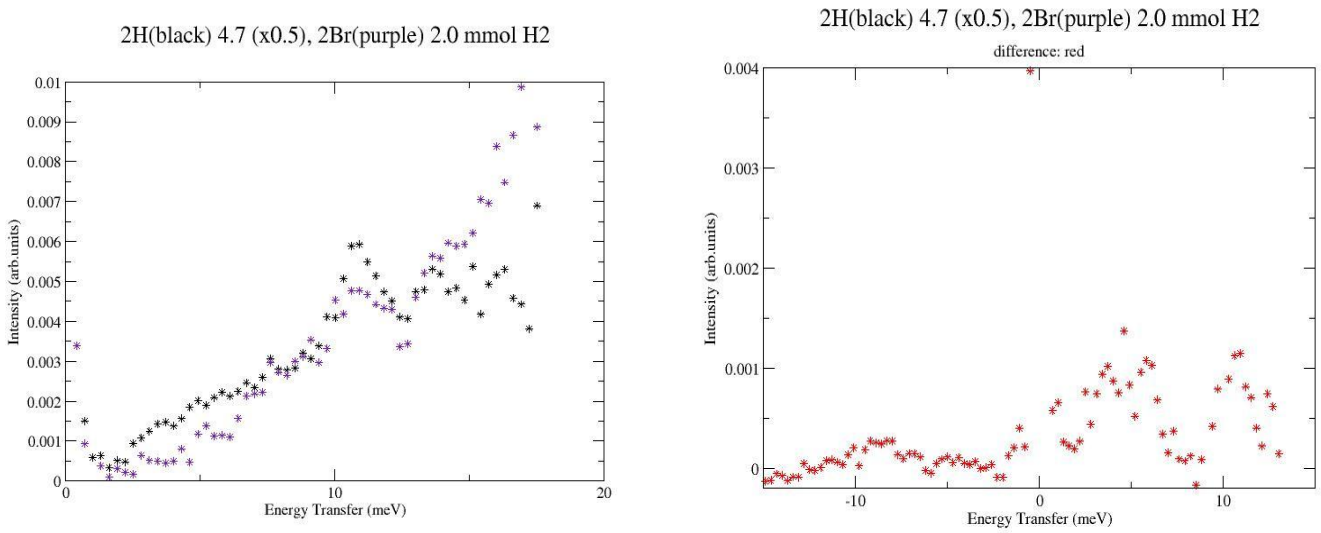

Figure S4. Spectra of (scaled) 4.7 mmol H_2 in **NU-301** (2H), and 2 mmol H_2 in **NU-302 (2Br) (**left) and difference spectrum (right): peaks at ~3.5, 6 and 10.5 meV, less well resolved on the energy gain side (left). The peak at 4 meV was confirmed in separate high-resolution spectra collected with 3.7 Å neutrons.

Table S6. Samples, actual amounts loaded into sample can, and hydrogen loadings used.

MOF	**mmol H_2**	**Weight Percent**
NU-301 (2H-BTBA)		
1.8g (1.6 mmol formula units)	2.3 mmol H_2	0.25 wt%
	4.7 mmol H_2	0.52 wt%
	8.7 mmol H_2	0.97 wt%
	22 mmol H_2	2.4 wt%
NU-302 (2Br-BTBA)		
1.0g (0.75 mmol formula units)	2 mmol H_2	0.4 wt%
	10 mmol H_2	2.0 wt%
0.6 g (0.45 mmol formula units)	3 mmol H_2	1.0 wt%

References

(1) Kresse, G.; Furthmuller, J. *Comput. Mater. Sci.* **1996**, *6*, 15.
(2) Blochl, P. E. *Phys. Rev. B* **1994**, *50*, 17953.
(3) Kresse, G.; Joubert, D. *Phys. Rev. B* **1999**, *59*, 1758.
(4) Perdew, J. P.; Burke, K.; Ernzerhof, M. *Phys. Rev. Lett.* **1996**, *77*, 3865.
(5) Monkhorst, H. J.; Pack, J. D. *Phys. Rev. B* **1976**, *13*.
(6) Manz, T. A.; Sholl, D. S. *J. Chem. Theory Comput.* **2010**, *6*, 2455.
(7) Dubbeldam, D.; Calero, S.; Ellis, D. E.; Snurr, R. Q.; RASPA 1.0; Northwestern University: Evanston, IL, 2008.
(8) Mayo, S. L.; Olafson, B. D.; Goddard, W. A. *Journal of Physical Chemistry* **1990**, *94*, 8897.
(9) Michels, A.; Degraaff, W.; Tenseldam, C. A. *Physica* **1960**, *26*, 393.
(10) Darkrim, F.; Levesque, D. *Journal of Chemical Physics* **1998**, *109*, 4981.
(11) Garberoglio, G.; Skoulidas, A. I.; Johnson, J. K. *J. Phys. Chem. B* **2005**, *109*, 13094.
(12) Duren, T.; Bae, Y.-S.; Snurr, R. Q. *Chem. Soc. Rev.* **2009**, *38*, 1237.
(13) Matanovic, I.; Belof, J. L.; Space, B.; Sillar, K.; Sauer, J.; Eckert, J.; Bacic, Z. *J. Chem. Phys.* **2012,** *137*, 14701.
(14) Nicol, J. M.; Eckert, J.; Howard, J. *J. Phys. Chem. B* **1988**, *92,* 7117.
(15) Rowsell, J. L. C.; Yaghi, O. *Angew. Chem., Int. Ed.* **2005**, *44*, 4670.
(16) Nouar, F.; Eckert, J.; Eubank, P. F.; Eddaoudi, M. *J. Am. Chem. Soc.* **2009**, *131*, 2864.
(17) Eckert, J.; Trouw, F. R.; Mojet, B.; Forster, P. M.; Lobo, R. *J. Nanosci. Nanotech.* **2009**, *9*, 1.